

Neurons Generated by Mouse ESCs with Hippocampal or Cortical Identity Display Distinct Projection Patterns When Co-transplanted in the Adult Brain

Marco Terrigno,¹ Irene Busti,^{2,3} Claudia Alia,³ Marta Pietrasanta,³ Ivan Arisi,⁴ Mara D'Onofrio,⁴ Matteo Caleo,^{3,5} and Federico Cremissi^{1,5,*}

¹Scuola Normale Superiore, Pisa 56126, Italy

²Neurofarba, University of Florence, Florence 50134, Italy

³Istituto di Neuroscienze, CNR, Pisa 56124, Italy

⁴European Brain Research Institute (EBRI) "Rita Levi-Montalcini", Roma 00161, Italy

⁵Co-senior author

*Correspondence: federico.cremisi@sns.it

<https://doi.org/10.1016/j.stemcr.2018.01.010>

SUMMARY

The capability of generating neural precursor cells with distinct types of regional identity *in vitro* has recently opened new opportunities for cell replacement in animal models of neurodegenerative diseases. By manipulating Wnt and BMP signaling, we steered the differentiation of mouse embryonic stem cells (ESCs) toward isocortical or hippocampal molecular identity. These two types of cells showed different degrees of axonal outgrowth and targeted different regions when co-transplanted in healthy or lesioned isocortex or in hippocampus. In hippocampus, only precursor cells with hippocampal molecular identity were able to extend projections, contacting CA3. Conversely, isocortical-like cells were capable of extending long-range axonal projections only when transplanted in motor cortex, sending fibers toward both intra- and extra-cortical targets. Ischemic damage induced by photothrombosis greatly enhanced the capability of isocortical-like cells to extend far-reaching projections. Our results indicate that neural precursors generated by ESCs carry intrinsic signals specifying axonal extension in different environments.

INTRODUCTION

In recent years, the use of pluripotent stem cells has allowed the production of neurons with specific identities. This has been made possible by the modification of existing methods of *in vitro* neuralization and patterning of pluripotent cells, by fine-tuning the signaling pathways that normally orchestrate the acquisition of distinct types of neuronal identities during embryonic brain development (Hansen et al., 2011; Lupo et al., 2014). The ability to obtain virtually any particular type of neuronal identity starting from pluripotent cell cultures has generated new expectations of feasible and reliable protocols of neuronal cell transplantation for the potential treatment of many different neurodegenerative diseases. In fact, neurons suitable for transplantation must be able to integrate into the host tissue, produce the appropriate type of neurotransmitter and neurotransmitter receptors, and develop functional synapses with the host neurons. All these capabilities are normally displayed by *in vitro* produced neurons (Espuny-Camacho et al., 2013; Michelsen et al., 2015; Yu et al., 2014). However, a crucial requirement for successful transplants is the ability of transplanted neurons to generate specific connections with functionally relevant targets.

So far, the regional identity of the neurons produced *in vitro* through the neuralization of pluripotent cells has mainly been established by their molecular charac-

terization through variable degrees of analysis of their neurotransmitter phenotype (Eiraku et al., 2011; Shi et al., 2012; Shiraishi et al., 2017; Yu et al., 2014) to a deeper investigation of their molecular nature by methods of global gene expression analysis (Bertacchi et al., 2013, 2015a, 2015b; Edri et al., 2015; Espuny-Camacho et al., 2013; Van de Leemput et al., 2014; Yao et al., 2017). Even so, ascertaining the identity of a nerve cell produced *in vitro* by comparison of its global gene expression profile with that of neurons *in vivo* is very useful but not sufficient. Indeed, the expression of markers of different positional identities in the CNS often depends on the developmental time of the analysis, thus making a given combination of markers specific to a type of neural cell only in a narrow time window.

A crucial aim for cell replacement protocols is the ability to produce the wanted type of neural cell to be replaced. The molecular identity of a neural cell by itself might not be predictive of its ability to extend appropriate projections and contact the right targets once transplanted *in vivo*, and the adult brain is the favorite host structure for assaying this ability in transplantation experiments. Isocortex and hippocampus are main targets of neurodegenerative diseases, thus making them attractive candidates for cell replacement studies (Iqbal et al., 2015; Poewe et al., 2017). The hippocampus is a natural niche of adult neurogenesis and a source of

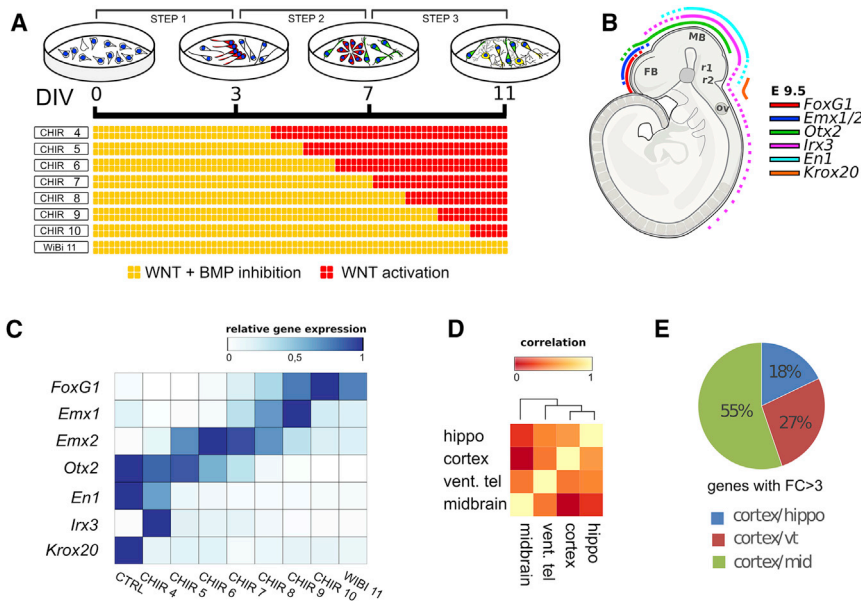


Figure 1. Timely Regulation of Wnt and BMP Signaling Affects the Regional Identity of ESC-Derived Neurons

(A) Scheme of the ESC differentiation protocol. DIV, days of *in vitro* differentiation. (B) Schematic drawing of an E9.5 embryo with the domains of expression of A/P markers.

(C) Color map shows the mRNA fold change of the A/P markers in (B), as evaluated by RT-PCR in ESC-derived neurons. $n = 3$ independent experiments were pooled together and analyzed by qRT-PCR; each experiment contained $n = 2$ *in vitro* technical replicates. (D and E) Global gene expression analysis of embryonic E15.5 regions: isocortex, hippocampus, midbrain, and ventral telencephalon. Explants from three embryos were pooled together. (D) Color map showing hierarchical clustering analysis of the distribution of Pearson correlation among transcriptome subsets of different embryonic brain regions.

The subset of transcriptome analyzed consists of the 487 genes with the highest variance among samples (top 2%). Ctx, isocortex; hip, hippocampus; mes, mesencephalon; vt, ventral telencephalon. (E) Pie chart reporting the % of genes with a 3-fold differential expression between isocortex and the other embryonic regions.

newly formed neurons that are capable of forming new connections in adult brain (Eriksson et al., 1998; Van Praag et al., 2002). This makes hippocampus the region of choice to assay the ability of *in vitro* produced neural cells to make projections and to send them to appropriate targets. Eventually, the similarity of the isocortex and hippocampus in terms of developmental origin makes the isocortex an ideal brain structure to be compared with hippocampus in transplantation studies.

In this work, we assayed the differential capability of neural cells obtained *in vitro*, which showed a molecular identity of precursor cells of isocortex or hippocampus, to generate long-range projections after transplantation in adult healthy or damaged brain. By a fine-tuning of Wnt and bone morphogenic protein (BMP) signaling during the *in vitro* differentiation of mouse embryonic stem cells (ESCs), we obtained neural precursor cells with global gene expression profile clustering with the profile of embryonic hippocampal or isocortical cells. When transplanted in adult healthy hippocampus, only hippocampal-like cells were able to extend long-range projections from the site of transplantation, contacting target regions that were appropriate for hippocampal neurons. Instead, when transplanted into healthy or damaged isocortex, isocortical-like cells were also capable of extending both cortical and extra-cortical far-reaching processes. Our study indicates that the molecular identity acquired *in vitro* by neuralized ESCs

dramatically affects their ability to form projections when transplanted in distinct brain regions.

RESULTS

Timely Manipulation of Wnt and BMP Signaling during Mouse ESC Neuralization Generates Neural Precursor Cells with a Molecular Isocortical or Hippocampal Identity

Wnt and BMP signaling profoundly affects the fate of prosencephalic cells. In fact, during development, their repression is first required for acquiring a dorsal telencephalic identity. Subsequently, the dorsal midline of the telencephalic vesicle invaginates, forming the median wall of the hem and the choroid plexus (Figure S1A). Secreted Wnt factors from the hem are necessary for establishing the hippocampal identity in the adjacent presumptive cortex (Lee et al., 2000; Machon et al., 2007). Therefore, we assayed the effect of inhibiting or activating the two signaling pathways during defined time windows of the ESC neuralization protocol (Figure 1A; DIV, days of *in vitro* neuralization).

Neuralizing ESCs required combined Wnt/BMP inhibition to acquire a dorsal telencephalic molecular identity (Bertacchi et al., 2015b; Yao et al., 2017). This is shown by the relative expression of anteroposterior (A/P) embryonic CNS markers (Figure 1B) in Wnt/BMP double-inhibited cells (WiBi cells) compared with control cells

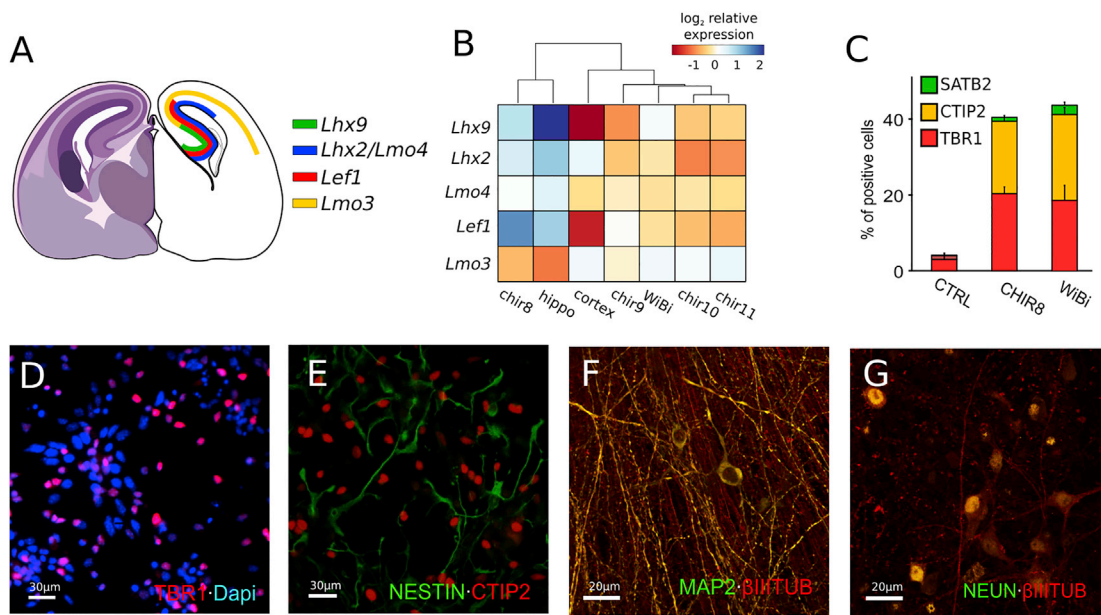


Figure 2. Wnt Signaling Manipulations Activate the Expression of Isocortical or Hippocampal Markers in Neuralized ESCs

(A) Schematic drawing of an E15.5 coronal section at the hippocampal level, showing the domains of expression of markers differentially expressed between isocortex and hippocampus.

(B) RT-PCR analysis of expression of the markers of hippocampal and isocortical identity shown in (A), in ESC-derived neurons. Color map show \log_2 mean-centered expression. $n = 3$ independent experiments were pooled together and analyzed by qRT-PCR; each experiment contained $n = 2$ *in vitro* technical replicates.

(C) Percentage of control (0.1% DMSO) and CHIR8 and WiBi cells positive for the dorsal telencephalic markers SATB2, CTIP2, and TBR1. Error bars, SD.

(D–G) Immunocytodetection (ICD) of different neuronal markers in CHIR8 cells. TBR1, CTIP2, and NESTIN: DIV13; β III TUBULIN, MAP2, and NEUN: DIV25.

(Figure 1C). Notably, double Wnt/BMP inhibition was no longer required after DIV8 to induce the expression of the telencephalic markers *FoxG1* and to repress the expression of the posterior markers *Irx3*, *Otx2*, *En1*, and *Krox20*. However, the reactivation of Wnt signaling from DIV8 by CHIR treatment (CHIR8 cells, Figure 1C) exerted a significant activation of *Emx1* and *Emx2* together with low expression of *Irx3*, *Otx2*, *En1*, and *Krox20*, and significant expression of *FoxG1*. Accordingly, CHIR treatments beginning before DIV8 (CHIR4–7) posteriorized the identity of cells, while CHIR treatments after DIV8 (CHIR9–10) were less effective in sustaining *Emx2* expression. *Emx1* and *Emx2* are expressed in a similar caudal-rostral gradient in the E9.5 embryonic cortex, both are highly expressed in the developing archicortex, and *Emx2* expression is crucial for hippocampal development (Fukuchi-Shimogori and Grove, 2003; Theil et al., 2002; Yoshida et al., 1997). Moreover, CHIR treatment before DIV8 (CHIR5–7) dramatically increased the expression of the markers of hem and choroid plexus *Lmx1a* and *Ttr* (Imayoshi et al., 2008; Kuwamura et al., 2005; Millonig et al., 2000), while decreasing the dorsal telencephalic marker

Lhx2 (Monuki et al., 2001; Subramanian et al., 2009) (Figures S1A and S1B).

Isocortex and hippocampus are two dorsal telencephalic structures with a common developmental origin and very similar profiles of gene expression. A main feature distinguishing them is the later development of hippocampus and its persistent neurogenesis in the adult. We performed gene expression profiling and compared the global gene expression of mouse E15.5 hippocampus, isocortex, midbrain, and ventral telencephalon. Accordingly, we found higher correlation of hippocampus and isocortex compared with midbrain or ventral telencephalon (Figures 1D and 1E).

A few markers of positional identity are known to be differentially expressed between embryonic hippocampus and isocortex (Abellán et al., 2014) (Figure 2A). The analysis of these markers (*Lhx2*, *Lhx9*, *Lmo3*, *Lmo4*, and *Lef1*) suggested a hippocampal rather than a posterior isocortical identity of CHIR8 cells (Figure 2B). In addition, CHIR-treated cells showed expression of the dorsal telencephalic markers TBR1, CTIP2, and SATB2 and TBR2 (Figures 2C–2E and S1C), as well as expression of the neuronal terminal

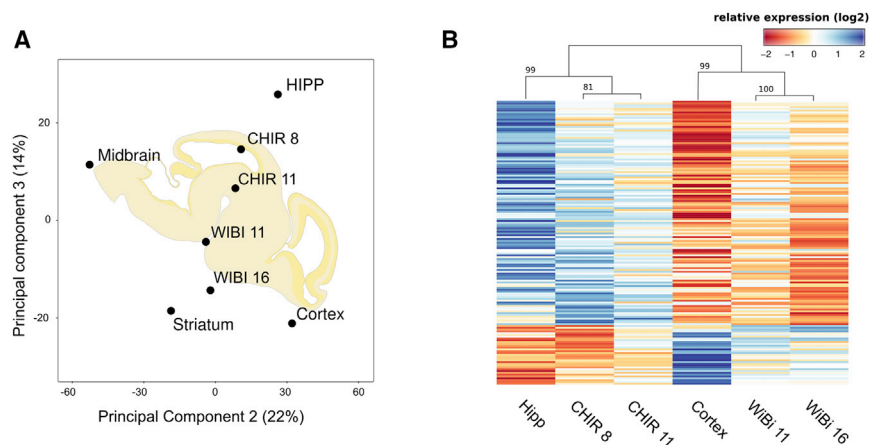


Figure 3. Wnt Signaling Induction or Repression Induce, Respectively, Hippocampal or Isocortical Global Gene Expression Profile in Neuralized ESCs

(A) PCA of the first quartile of most differentially expressed genes ($n = 3,145$) among WiBi cells, CHIR cells, and E15 embryonic regions shown in labels (see [Experimental Procedures](#)). $n = 3$ independent cell cultures or embryonic explants for each treatment/embryonic region were pooled together.

(B) Color map and hierarchical clustering (Pearson correlation) of the top 5% ($n = 157$) loadings of the third PCA component shown in (A). Clustering scores were computed via multiscale bootstrap resampling (pvclust, see [Experimental Procedures](#)). Scale indicates \log_2 mean-centered gene expression.

differentiation markers β III TUBULIN, NEUN, and MAP2 (Figures 2F and 2G). To further characterize the molecular identity of the cells in which Wnt/BMP signaling was continuously inhibited (WiBi cells) or cells in which Wnt/BMP signaling was reactivated from DIV8 (CHIR8 cells), we compared their global gene expression profiles with the profiles of embryonic cells by principal component analysis (PCA) and clustering analysis (Figures 3A and 3B). The second and the third components of PCA discriminated between E15.5 isocortex, striatum, hippocampus, midbrain, and cells treated with WiBi CHIR at different times. While WiBi-treated cells located closer to isocortex and striatum, CHIR-treated cells were closer to hippocampus (Figure 3A). Notably, the most significant loadings of the third component, which better separated hippocampus and isocortex, showed a significant clustering of WiBi and CHIR8 cells to E15.5 isocortex and hippocampus, respectively (Figure 3B). All in all, our results indicate that the differential activation from DIV8 of one single signaling, Wnt, induced a molecular identity of hippocampus (CHIR8 cells) instead of isocortex (WiBi cells).

Hippocampal Cells, but Not Isocortical Cells, Can Generate Long-Range Projections to Regions Targeted by Adult Dentate Gyrus Neurons, after Transplantation in Adult Hippocampus

We compared the behavior and projection pattern of the neural precursor cells produced via different Wnt/BMP signaling manipulation after grafting *in vivo*. First, we labeled WiBi and CHIR8 cells by lentiviral transduction with prenylated forms of EGFP and mCherry. Before transplantation, cells were treated with N-[N-(3,5-difluorophenacetyl)-L-alanyl]-S-phenylglycine t-butyl ester (DAPT) and AraC to force their differentiation and negatively select dividing progenitors, respectively (see [Experimental Pro-](#)

[cedures](#)). The two types of cells were first co-injected into the dentate gyrus (DG) of 2-month-old mice (Figure 4A), because this is a niche of adult neurogenesis (Eriksson et al., 1998; Van Praag et al., 2002), and it is also a permissive environment for the extension of new neuronal processes. Two months after injection, both WiBi and CHIR8 cells persisted in the host tissue (Figure 4B), showing expression of the terminally differentiated neuronal marker NEUN (Figures S2B and S2C). Importantly, 1 month after grafting, the proportions of NEUN/GFP and NEUN/Cherry double-positive cells in the transplant remained unchanged, suggesting an equal survival ratio for both cell types (Figure S2A). While isocortical cells were not able to extend long processes, only CHIR8 cells displayed abundant projections outside the graft, already 1 month after transplantation (Figures 4C–4G). These projections mainly contacted the ipsilateral CA3, CA1, subiculum, and entorhinal cortex (Figures 4C–4G). Fibers appeared to form potential synaptic contacts, as shown by staining with the vesicular glutamate transporter VGLUT1 (Figure S2D).

The density of the fibers reaching CA3 was significantly higher than the density of the fibers projecting to other hippocampal structures, especially when analyzed 2 months after grafting (Figures 4D and 4H). These observations were consistent with the capability of naive hippocampal cells to extend new long-range processes contacting CA3 during adult neurogenesis. Notably, 30.1% of transplanted CHIR8 cells expressed CALBINDIN1 (CALB1, Figures S3A and S3B), a marker for DG cells (Sloviter, 1989), 1 month after the transplantation. Moreover, most of the CHIR8 projections found in the Mossy Fiber pathway, which is a natural target of DG (Blackstad et al., 1970; Swanson et al., 1978; Gaarskjaer, 1978; Claiborne et al., 1986), were CALB1 positive (82.0%), while only 8.9% of the projections in CA1 expressed this marker

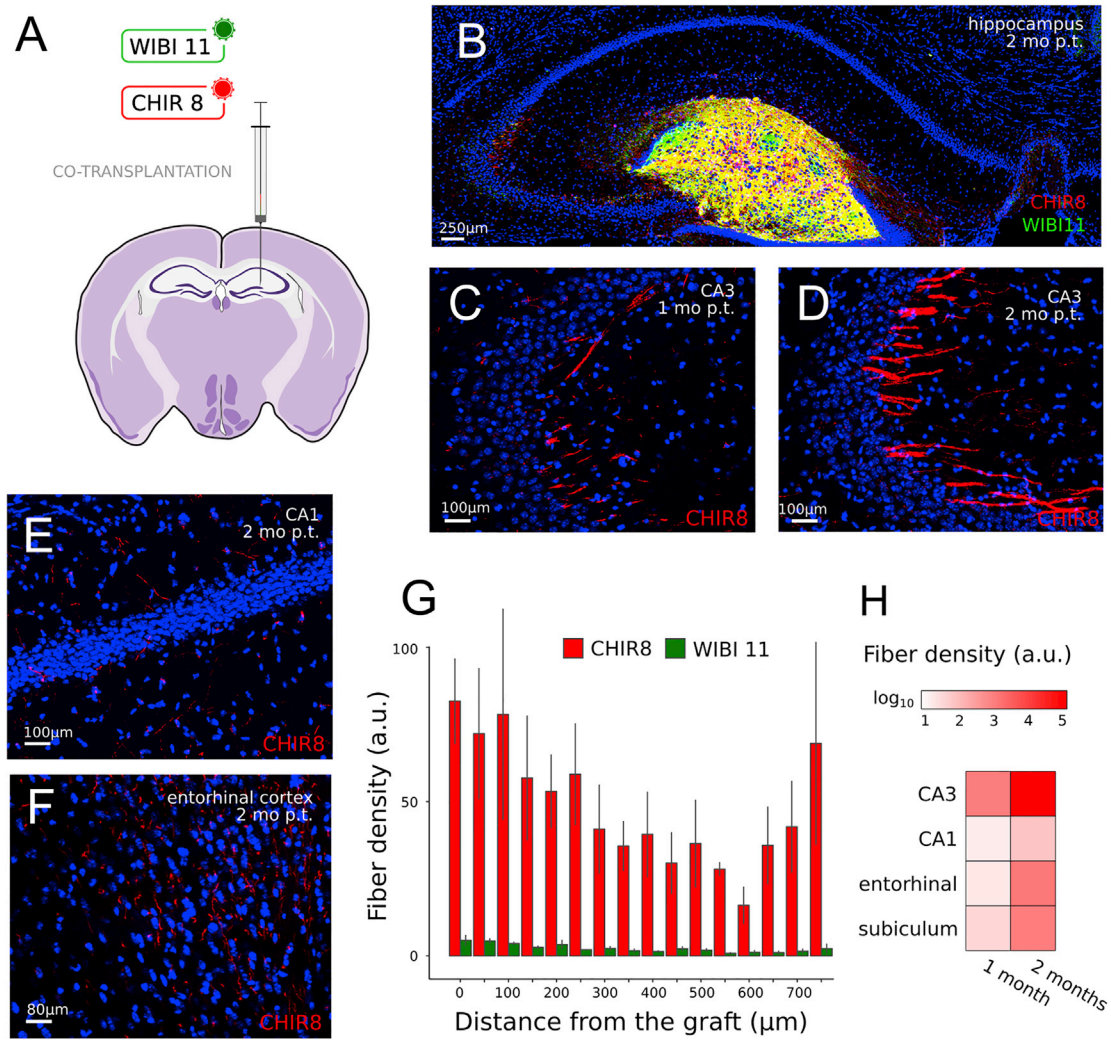


Figure 4. Cell Transplantation in Hippocampus

(A) Method and site of cell grafting.

(B) ICD of CHIR8 (red) and WiBi cells (green) 2 months post transplantation (mo p.t.) in hippocampus. Blue, Hoechst nuclear counterstaining.

(C–F) ICD of CHIR8 and WiBi fibers at different times post transplantation and in different regions, as indicated by labels.

(G) Density of WiBi and CHIR8 fibers at different distances from the graft, 1 month after transplantation. Error bars, SD.

(H) Heatmap of CHIR8 fiber density in different hippocampal regions 1 and 3 months after cell grafting. $n \geq 3$ transplanted animals for each time point were analyzed.

(Figures S3C–S3G). Overall, 88.4% of the CHIR8/CALB1 double-positive projections were found in the Mossy Fibers (Figure S3H). This result suggested that at least a subpopulation of CHIR8 cells displays DG identity and retains the projection pattern of endogenous DG cells.

Isocortical Cells Can Send Far-Reaching Projections When Transplanted in Adult Motor Cortex

When transplanted into adult motor cortex (Figure 5A), both WiBi and CHIR8 cells persisted at least 2 months after injection, and their ratio remained unchanged (Figures 5B

and S2E–S2G). As in the case of transplantations in hippocampus, CHIR8 cells were able to efficiently extend projections, either inside the cortex (Figures 5C–5F, 5H, 5I, 5K, and 5L) or toward extra-cortical regions (Figures 5G, 5J, and 5M). WiBi cells transplanted in adult motor cortex were also able to extend processes. However, they generated far-reaching processes less efficiently than CHIR8 cells 1 month after transplantation (Figures 5C–5J). Interestingly, 2 months after grafting, WiBi cells were even more effective than CHIR8 cells in extending processes within the motor cortex (Figures 5K and 5L) and almost as efficient

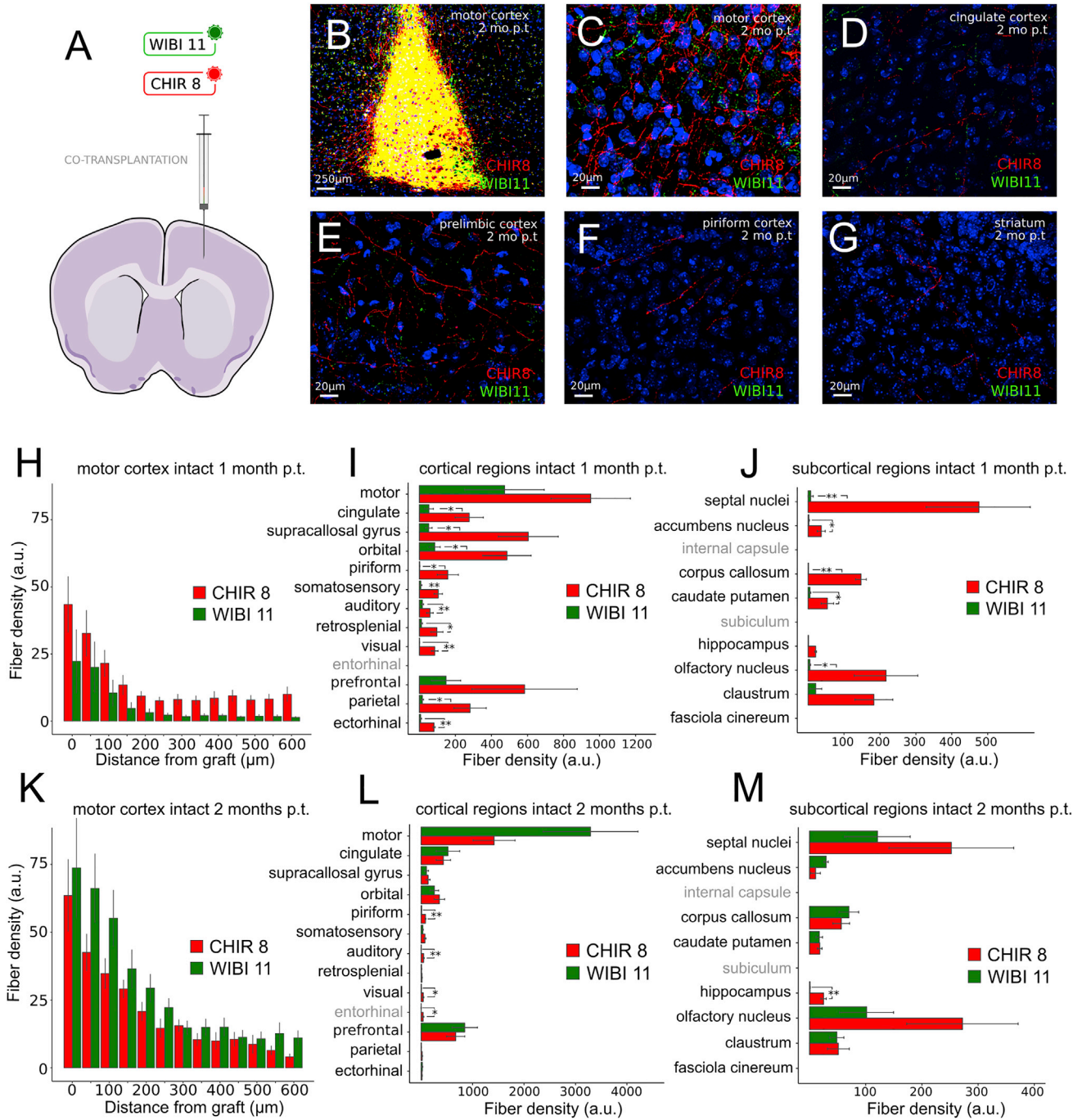


Figure 5. Cell Transplantation in Normal Motor Cortex

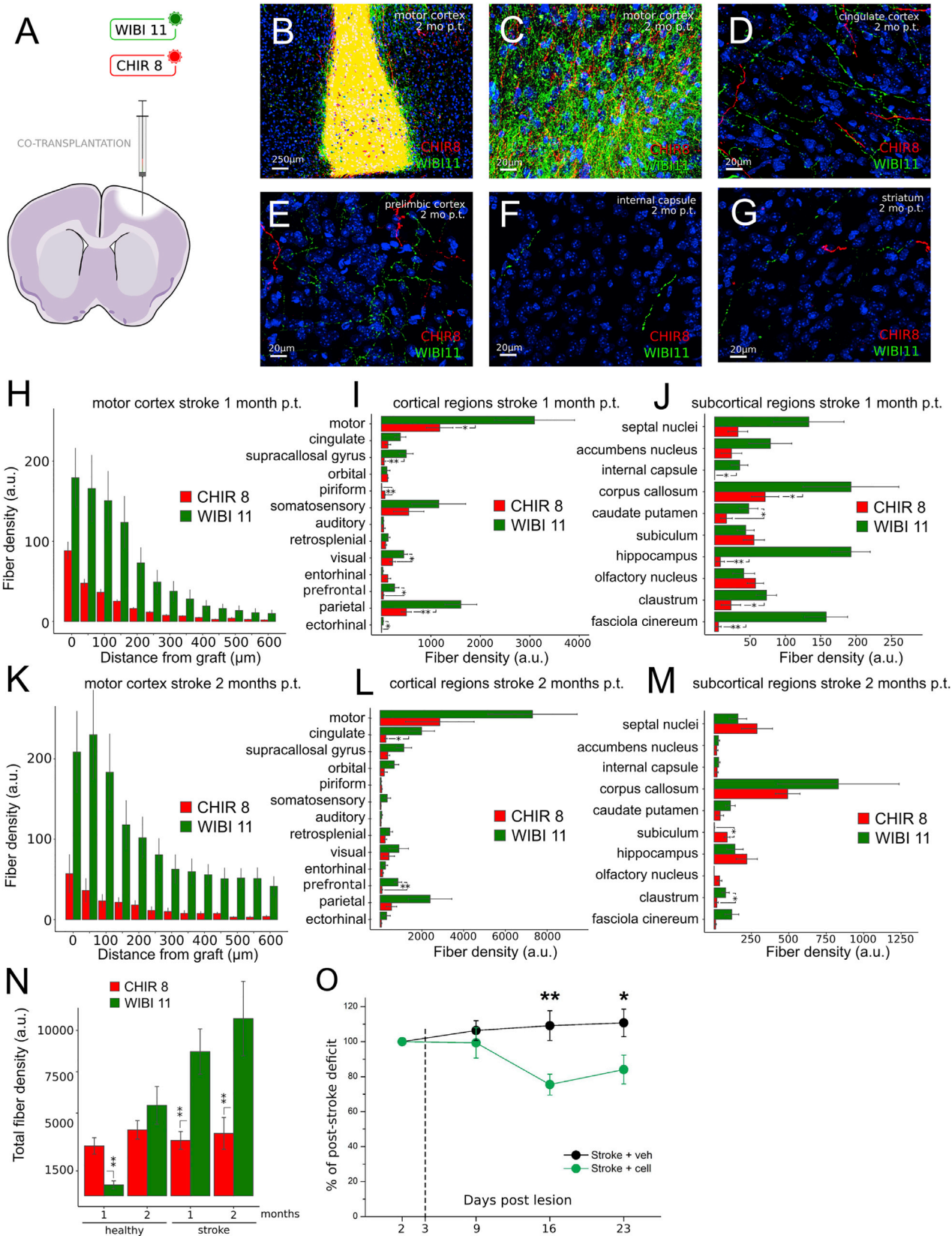
(A) Scheme of transplantation.

(B) ICD of CHIR8 (red) and WiBi cells (green) 2 months after transplantation in healthy motor cortex. Blue, Hoechst nuclear counter-staining.

(C–G) ICD of CHIR8 and WiBi fibers at different times post transplantation and in different regions, as indicated by labels.

(H and K) Density of WiBi and CHIR8 fibers at a different distances from the graft, 1 (H) and 2 months (K) after transplantation.

(I, J, L, and M) WiBi and CHIR8 fiber density in cortical (I and L) and extra-cortical (J and M) regions, 1 (I and J) and 2 months (L and M) after transplantation; Error bars, SD. * $p < 0.05$; ** $p < 0.01$ (two-tailed Student's t test). $n \geq 3$ transplanted animals for each time point were analyzed.



(legend on next page)



as them in sending axons to extra-cortical targets (Figure 5M). Specifically, while WiBi and CHIR8 cells shared most of the cortical and subcortical targets, some regions, such as the piriform cortex ($p < 0.01$), the auditory cortex ($p < 0.01$), the visual cortex ($p < 0.05$), the entorhinal cortex ($p < 0.05$), and the hippocampal formation ($p < 0.01$), were mostly targeted by CHIR8 cells (Figures 5L and 5M), indicating cell-specific axonal outgrowth. We also analyzed other subcortical targets, including the thalamus, midbrain, and corticospinal tract, but we could not detect significant projections for either cell type.

Altogether, these results indicated that cortical cells are slower than hippocampal cells in extending far-reaching axons when transplanted into the isocortex.

One important issue is whether the projection patterns of ESC-derived neurons resemble those of hippocampal and cortical cells derived from mouse embryos. To this aim, we co-transplanted fetal (E15.5) cortical and hippocampal neurons into the hippocampus (Figures S4A–S4F) or motor cortex (Figures S5A–S5F) of adult mice. We found that embryonic cells displayed similar patterns of projection compared with ESC-derived neurons, 1 month after transplantation. The main similarity concerned the differential projection pattern after transplantation into hippocampus. Indeed, only embryonic hippocampal, but not cortical cells, extended abundant projections and contacted CA3 via the Mossy Fiber pathway after grafting into the DG (Figures S4D and S4E).

Phot thrombotic Damage Dramatically Enhances the Ability of Isocortical Cells to Extend Long-Range Projections

To assay the impact of a brain lesion on the projections of transplanted cells, we grafted WiBi and CHIR8 cells in a mouse model of ischemic stroke in the motor cortex. Cells were injected 3 days after inducing phot thrombotic damage (Figure 6A; see [Experimental Procedures](#)) and their survival and pattern of axonal connectivity were analyzed

1 and 2 months after stroke (Figures 6B–6N). Both WiBi and CHIR8 cells integrated into the host tissue and were detectable at least 2 months after transplantation (Figures 6B, S2E, S2H, and S2I). As when transplanted in healthy motor cortex, CHIR8 cells efficiently extended axons into both cortical and extra-cortical regions, 1 month (Figures 6H–6J) and 2 months (Figures 6K–6M) after transplantation. However, WiBi cells formed intra-cortical projections more efficiently than CHIR8 cells already 1 month after grafting (Figures 6H and 6I). This was paralleled by an enhanced ability of WiBi cells to target subcortical regions 1 month after transplantation (Figure 6J). However, 2 months after grafting, a refinement of axonal targeting occurred, making CHIR8 projections into septal nuclei and hippocampus more abundant than WiBi projections (Figures 6M and 7). Finally, the different behavior of WiBi and CHIR8 cells was even more striking considering the total amount of fibers in all the regions analyzed (Figure 6N). Interestingly, CHIR8 cells appeared to reach a plateau in projection density already 1 month after transplantation, and the total amount of fibers was not influenced by the ischemic insult, while WiBi cell projections increased with time and were specifically promoted by the lesion. We concluded that the phot thrombotic damage further enhanced the process extension of WiBi cells, but CHIR8 and WiBi cells retained their cell-autonomous ability to project toward specific cortical and extra-cortical targets.

We also asked whether cell grafting had an impact on motor performance in animals with ischemic damage. We chose to implant WiBi cells since they showed better long-term integration than CHIR8 cells in our stroke model (Figures 6N and 7). Thus, mice received WiBi cell transplantation 3 days after experimental stroke, and motor function was assessed longitudinally via the gridwalk test (Lai et al., 2015; Alia et al., 2016). We found that while the motor deficit remained stable in the mice treated with vehicle solution, grafted mice showed a decline (starting from 16 days post stroke) in the number of foot faults made

Figure 6. Cell Transplantation in the Ischemic Motor Cortex

(A) Method and site of transplantation.

(B) ICD of CHIR8 (red) and WiBi (green) cells 2 months after transplantation in phot thrombotic motor cortex. Blue, Hoechst nuclear counterstaining.

(C–G) ICD of CHIR8 and WiBi fibers at different times post transplantation and in different regions, as indicated by labels.

(H and K) Density of WiBi and CHIR8 fibers at different distances from the graft, 1 (H) and 2 months (K) after transplantation.

(I, J, L, and M) WiBi and CHIR8 fiber density in cortical (I and L) and extra-cortical (J and M) regions, 1 (I and J) and 2 months (L and M) after transplantation. Error bars, SD.

(N) Total fiber density of WiBi and CHIR8 cells in healthy and ischemic brains, 1 and 2 months after grafting. (I, J, and L–N) * $p < 0.05$; ** $p < 0.01$ (two-tailed Student's *t* test); $n \geq 3$ transplanted animals for each time point were analyzed.

(O) Percentage of foot faults made with the contralesional forelimb in the gridwalk test. Values were normalized on the 2 days post stroke value (initial deficit before transplantation). After the injection of WiBi cells (green, $n = 9$) at day 3, mice showed a significant improvement in the motor performance compared with mice injected with vehicle (black, $n = 5$) (two-way repeated-measures ANOVA followed by Holm-Sidak test: 16 days, ** $p = 0.004$; 23 days, * $p = 0.015$). Error bars, SD.



induced in neural precursor cells generated by human iPSCs that were initially deprived of Wnt/BMP signaling and then exposed to exogenous Wnt/BMP. Moreover, they showed that the neurons generated in this way were able to functionally integrate into mouse DG after grafting, suggesting that Wnt/BMP signaling was required to induce a hippocampal identity in precursor cells that were previously committed to a general telencephalic identity. However, a direct comparison of these cells with different cells, focusing on the capacity to integrate and extend neurites in distinct environments, was not performed.

We aimed to precisely identify the molecular identity of our *in vitro* generated neural progenitor and precursor cells. The analysis of specific markers of hippocampal versus isocortical differentiation, and the comparison of the global gene expression profiles of *in vitro* differentiated cells and of a number of embryonic regions, allowed us to identify a mechanism that is sufficient to refine the dorsal telencephalic positional differentiation. Our results indicate that in a specific time window, which corresponds to DIV8 of our protocol of neuralization, cells can acquire either an isocortical or a hippocampal molecular identity, depending on the degree of Wnt signaling at that time. Markers that show that graded expression levels between the embryonic hippocampus (*Lhx9*, *Lhx2*, *Lef1*, *Lmo4*) and isocortex (*Lmo3*) were differentially expressed by WiBi and CHIR8 cells. Moreover, the global gene expression profiles of WiBi and CHIR8 cells clustered with embryonic isocortex and hippocampus, respectively. Wnt signaling de-inhibition before DIV8, or later than DIV9, failed to induce a hippocampal gene expression profile, indicating the existence of a time window of cellular competence for the induction of hippocampal identity.

It is known that hippocampal cells, together with olfactory bulb cells, are the only CNS cells able to undergo efficient adult neurogenesis in mammals (Eriksson et al., 1998; Van Praag et al., 2002). Conversely, adult cortical cells are not able, in physiological conditions, to generate new neurons, although they share common origin and similar molecular identity with hippocampal cells (Magavi et al., 2000). In this study, we compared WiBi and CHIR8 cells for their ability to generate new processes in different *in vivo* environments. To this aim, we compared their pattern of connectivity by differentially labeling them with fluorochrome-carrying lentiviral vectors and co-transplanting them into different adult brain regions.

Both WiBi and CHIR8 precursors survived and fully differentiated in mature neurons after grafting in adult hippocampus and isocortex. However, they showed different capacity for axonal projection. In intact hippocampus, only grafted hippocampal cells were able to extend long-range projections, while isocortical cells failed in sending far-reaching processes. At least a subpopulation

(about 30%) of CHIR8 cells displayed markers of DG granule cells, such as CALB1, and contacted proper targets of adult DG neurons, such as CA3. This axonal projection became more robust over time, as shown by the dramatic enhancement of fiber density 2 months versus 1 month after transplant (Figure 4H). Finally, the fact that similar results were obtained when transplanting primary cultures of fetal hippocampal or cortical neurons suggests that the different behavior of CHIR8 and WiBi cells might indeed be due to the specific respective hippocampal and cortical identity acquired *in vitro*.

Likewise fetal cells of the embryonic motor cortex, ESC-derived isocortical cells transplanted into either intact or photothrombotic motor cortex failed in sending projections to thalamic nuclei and midbrain, according to previous observations (Michelsen et al., 2015). In addition, a significant number of processes were found in the internal capsule of photothrombotic brains 1 month after stroke. Based on these observations, we might speculate that our cells acquired a motor identity. However, we cannot exclude that they might simply have maintained a general isocortical identity and that a further specification step would have been required to generate also thalamic and midbrain projections. Their layer identity remains to be assessed, but we speculate that a majority of them differentiated as deep-layer neurons, because at the time of their transplantation they were mostly expressing TBR1 and CTIP2 markers (Figure 2C).

The results obtained after transplantation in photothrombotic motor cortex indicate that the normal cortical environment retains some cues inhibiting the extension of new processes from WiBi cells and that such cues are somehow removed after the photothrombotic damage. However, it is interesting to note that, after a first early phase when WiBi processes were much denser than CHIR8 processes both in cortical and extra-cortical regions 1 month after grafting, 2 months after, the density of CHIR8 fibers in hippocampus and septal nuclei was significantly higher than the density of WiBi processes. We speculate that, in addition to a differential capacity of axonal extension, WiBi and CHIR8 cells hold some ability in selecting specific targets of innervation that is refined over time. This is also supported by the observation that WiBi processes were less dense than CHIR8 processes in healthy motor cortex and callosum 1 month after graft, but they increase dramatically at 2 months. These data suggest that isocortical and hippocampal cells display different degrees of axonal pruning/plasticity in specific brain regions.

Altogether, our observations indicate that the distinct molecular identities acquired by CHIR8 and WiBi cells paralleled their different behavior after transplantation and suggest that WiBi and CHIR8 cells might be very similar to naive isocortical and hippocampal precursor cells,



respectively. Furthermore, this interpretation is supported by the similar projection patterns established by fetal hippocampal and cortical neurons co-transplanted under the same experimental conditions as WiBi/CHIR8 cells (see [Figures S4 and S5](#)).

Fetal hippocampal cells grafted into the adult mouse hippocampus survived and successfully contacted the correct hippocampal layers and typical hippocampal target regions as the septum and the entorhinal cortex ([Shetty and Turner, 1996](#); [Zaman and Shetty, 2001](#)). In addition, mouse and human neurons generated *in vitro* by pluripotent cells were also successfully grafted into mouse hippocampus ([Yu et al., 2014](#)) or hippocampal slice ([Hiragi et al., 2017](#)). Consistently, we observed a very similar pattern of connectivity after transplantation of both fetal or ESC-derived neurons in hippocampus.

A number of experiments of grafting into mouse isocortex of either fetal cells or neural precursors originated *in vitro* by pluripotent cells have been performed. Overall, these studies show that embryonic or fetal neural precursors transplanted in the intact adult hippocampus integrate efficiently in the host circuitry and contact the correct target in the host tissue displaying specific patterns of long-range projections, whereas the intact adult cortical parenchyma appears to be poorly permissive with the transplanted cells ([Avaliani et al., 2014](#); [Fricker-Gates et al., 2002](#); [Gage et al., 1995](#); [Guitet et al., 1994](#); [Rosario et al., 1997](#); [Sheen et al., 1999](#); [Shetty and Turner, 1996](#); [Shin et al., 2000](#)). Indeed, this behavior suits well with the natural capability of the hippocampal niche, unlike the cortical environment, to support adult neurogenesis. In addition, several studies reported that experimentally induced cortical damage (e.g., aspiration, experimental ischemia, or chemically induced neurodegeneration) resulted in functional integration and higher connectivity of the transplanted cells, thus suggesting the existence of inhibitory cues in the healthy isocortex removed by the lesion ([Espuny-Camacho et al., 2013](#); [Falkner et al., 2016](#); [Gaillard et al., 2007](#); [Michelsen et al., 2015](#); [Torner et al., 2013](#)). Our results, which are consistent with these observations, indicate that the inhibitory effect of the intact cortical environment affects isocortical but not hippocampal cells, both fetal or originating from ESCs, although the signals mediating such inhibition are currently unknown.

The possibility to successfully transplant neural precursors originated *in vitro* from ESCs or iPSCs into damaged isocortex has opened new opportunities for therapeutic approaches for cortical stroke. Here, we showed that transplanted cells were able to establish potential synaptic connections with the host, as indicated by axonal varicosities stained with VGLUT1 ([Figures S2D and S2J](#)). Moreover, grafting WiBi cells promoted some functional restoration of forelimb function after ischemic damage to the motor

cortex. Improvements in motor output were already apparent as early as 16 days after stroke, suggesting that, in addition to network rewiring due to axon extension by the transplanted cells, bystander effects (e.g., release of trophic factors, modulation of inflammation; [George and Steinberg, 2015](#); [Lee et al., 2008](#); [Chen et al., 2003](#); [Borlongan et al., 1998](#); [Modo et al., 2002](#)) likely play a key role in the observed recovery. Finally, we speculate that the specificity of innervation that we found for WiBi and CHIR8 cells might affect later processes of motor recovery. These and other functional aspects of cell transplantation in ischemic motor cortex are currently under investigation.

Our results highlight the importance of the type of molecular identity acquired by the cells during their *in vitro* neuralization to establish proper connections. When transplanted into photothrombotic motor cortex, WiBi cells, more efficiently than CHIR8 cells, sent far-reaching processes toward the surrounding cortical regions (somatosensory, cingulate, prefrontal) and some subcortical regions (internal capsule, caudate putamen, claustrum) typically targeted by resident cortical projection neurons. Although our observations clearly indicate a functional difference between WiBi and CHIR8 cells, we cannot anticipate how their differential connectivity after grafting could relate to their different molecular identity. The analysis of genes differentially expressed between hippocampal and isocortical cells originating from ESCs *in vitro* showed clusters of biologically related pathways with high enrichment score comprising extracellular matrix (ECM)-cell interaction (the most enriched), cell-cell interaction, PI3K-Akt signaling pathway, and WNT signaling. Notably, ECM-cell interaction is also the most enriched pathway in the analysis of genes differentially expressed between embryonic isocortex and hippocampus ([Table S1](#)). We speculate that changed expression of some of the genes belonging to this category could account for the specificity of connectivity of WiBi and CHIR8 cells.

In conclusion, our *in vitro* system proved useful to finely dissect the molecular pathways generating cell diversity in CNS development. *In vivo* grafting in distinct adult brain regions revealed an intrinsic functional diversity of neural precursor cells generated *in vitro*, which might have a crucial impact for cell replacement therapies. Our findings support the importance of *in vitro* systems in addressing developmental biology issues and pose the bases for more focused assays of isocortical or hippocampal cell replacement.

EXPERIMENTAL PROCEDURES

Cell Culture

Murine ESC lines E14Tg2A (passages 25–38) were cultured as described ([Bertacchi et al., 2013](#); [Lupo et al., 2014](#)). For their differentiation, ESCs were seeded on gelatin-coated culture dishes



(65,000 cells per cm²; DIV0) and cultured in chemically defined minimal medium (CDMM: DMEM/F12 supplemented with N2/B27; see [Supplemental Information](#) for the exact composition) plus 2.5 μM Wnt inhibitor (53AH) and 0.25 μM BMP inhibitor (LDN193189) for 3 days. At DIV3, cells were dissociated and seeded (65,000 cells per cm²) on poly-ornithine and natural mouse Laminin. Cells were cultured for 4 additional days in CDMM plus Wnt/BMP inhibitors. At DIV7, cells were dissociated and seeded (125,000 cells per cm²) on poly-ornithine and Laminin-coated wells. Subsequently, isocortical cultures were kept in CDMM plus Wnt/BMP inhibitors (WiBi 11), whereas hippocampal cultures were grown in CDMM supplemented with CHIR 3 μM (CHIR8) for 4 additional days. At DIV11, DMEM/F12 was replaced with Neurobasal to avoid glutamate-induced excitotoxicity.

Gene Expression

RT-PCR and immunocytochemistry (ICD) analyses were carried out as previously described ([Bertacchi et al., 2013](#)). An Agilent SurePrint G3 Mouse Gene Expression Array (8 × 60 K, grid ID 028005) was hybridized and analyzed as described ([Bertacchi et al., 2015a](#)).

In Vivo Grafting

Animal protocols were reviewed and approved by the Italian Ministry of Health, authorization 739/2017-PR. The photothrombotic lesion was induced as previously described ([Lai et al., 2015](#); [Alia et al., 2016](#)). WiBi- and CHIR-treated neurons were transduced at DIV9, respectively, with a lentivirus carrying a membrane-bound form of GFP or mCherry. Lentiviral vectors were constructed swapping the original GFP in the pWPXLd vector (Addgene number 12258) with, respectively, the prenylated GFP in pME-EGFP-CAAX and mCherry in pME-mCherry-CAAX (Tol2kit, [Kwan et al., 2007](#)). To eliminate undifferentiated ESCs and cycling cells, gamma-secretase inhibitor 10 μM (DAPT) was added to the culture medium on days 14 and 15 and Aracytin 5 μM (AraC) on day 15. At DIV16, ESCs were dissociated and resuspended at a concentration of 150,000 cells/μL in DMEM/F12 supplemented with 10% fetal calf serum. In co-transplantation experiments, WiBi- and CHIR-treated cells were pooled and injected together in equal proportions. A volume of 1 μL of cell suspension was injected in 2-month-old mice. The gridwalk test was employed for the behavioral assessment of motor deficits after ischemia ([Lai et al., 2015](#)).

Imaging

Z-stack images (2.5-μm z-step size) of three different sections were acquired with the ZENpro software (Zeiss) and then processed with ImageJ 1.48p software (<https://imagej.nih.gov/ij/index.html>). Projection density was calculated as the total number of pixels above threshold normalized on the average area (expressed in millions of pixels) of the graft from which the fibers originated.

Detailed experimental procedures are available in the [Supplemental Information](#).

ACCESSION NUMBERS

The accession number for the microarray gene expression data reported in this paper is GEO: GSE108466.

SUPPLEMENTAL INFORMATION

Supplemental Information includes Supplemental Experimental Procedures, five figures, and one table and can be found with this article online at <https://doi.org/10.1016/j.stemcr.2018.01.010>.

AUTHOR CONTRIBUTIONS

M.T., M.C., and F.C. designed experiments; M.T. performed cell culture, molecular biology, imaging, and gene expression data computation; I.B. and C.A. planned and carried out *in vivo* experimental activity and imaging; M.P. set up the cell transplantation protocol; M.D. designed and performed the microarray analysis; I.A. performed the microarray computational analysis; M.C. and F.C. wrote manuscript.

ACKNOWLEDGMENTS

This work was supported by University and Research grant PRIN-2102 (F.C.). This study was also supported by Regione Toscana (RONDA Project, “Programma Attuativo Regionale” financed by FAS, now FSC) and by the EU Commission, FP7 PAINCAGE Project, grant number 603191 and the H2020-ICT-2016 MADIA Project, grant number 732678.

Received: July 26, 2017

Revised: January 14, 2018

Accepted: January 15, 2018

Published: February 15, 2018

REFERENCES

- Abellán, A., Desfilis, E., and Medina, L. (2014). Combinatorial expression of Lef1, Lhx2, Lhx5, Lhx9, Lmo3, Lmo4, and Prox1 helps to identify comparable subdivisions in the developing hippocampal formation of mouse and chicken. *Front. Neuroanat.* 8, 59.
- Alia, C., Spalletti, C., Lai, S., Panarese, A., Micera, S., and Caleo, M. (2016). Reducing GABA A-mediated inhibition improves forelimb motor function after focal cortical stroke in mice. *Sci. Rep.* 6, 1–15.
- Avaliani, N., Sørensen, A.T., Ledri, M., Bengzon, J., Koch, P., Brüstle, O., Deisseroth, K., Andersson, M., and Kokaia, M. (2014). Optogenetics reveal delayed afferent synaptogenesis on grafted human-induced pluripotent stem cell-derived neural progenitors. *Stem Cells* 32, 3088–3098.
- Bertacchi, M., Pandolfini, L., Murenu, E., Viegi, A., Capsoni, S., Cellerino, A., Messina, A., Casarosa, S., and Cremisi, F. (2013). The positional identity of mouse ES cell-generated neurons is affected by BMP signaling. *Cell. Mol. Life Sci.* 70, 1095–1111.
- Bertacchi, M., Lupo, G., Pandolfini, L., Casarosa, S., D’Onofrio, M., Pedersen, R.A., Harris, W.A., and Cremisi, F. (2015a). Activin/nodal signaling supports retinal progenitor specification in a narrow time window during pluripotent stem cell neuralization. *Stem Cell Reports* 5, 1–14.
- Bertacchi, M., Pandolfini, L., D’Onofrio, M., Brandi, R., and Cremisi, F. (2015b). The double inhibition of endogenously produced



- BMP and Wnt factors synergistically triggers dorsal telencephalic differentiation of mouse ES cells. *Dev. Neurobiol.* 75, 66–79.
- Blackstad, T.W., Brink, K., Hem, J., and June, B. (1970). Distribution of hippocampal mossy fibers in the rat. An experimental study with silver impregnation methods. *J. Comp. Neurol.* 138, 433–449.
- Borlongan, C.V., Tajima, Y., Trojanowski, J.Q., Lee, V.M., and Sanberg, P.R. (1998). Cerebral ischemia and CNS transplantation: differential effects of grafted fetal rat striatal cells and human neurons derived from a clonal cell line. *Neuroreport* 9, 3703–3709.
- Bulfone, A., Smiga, S.M., Shimamura, K., Peterson, A., Puelles, L., and Rubenstein, J.L.R. (1995). T-Brain-1: a homolog of Brachyury whose expression defines molecularly distinct domains within the cerebral cortex. *Neuron* 15, 63–78.
- Chambers, S.M., Fasano, C.A., Papapetrou, E.P., Tomishima, M., Sadelain, M., and Studer, L. (2009). Highly efficient neural conversion of human ES and iPS cells by dual inhibition of SMAD signaling. *Nat. Biotechnol.* 27, 275–280.
- Chen, J., Li, Y., Katakowski, M., Chen, X., Wang, L., Lu, D., Lu, M., Gautam, S.C., and Chopp, M. (2003). Intravenous bone marrow stromal cell therapy reduces apoptosis and promotes endogenous cell proliferation after stroke in female rat. *J. Neurosci. Res.* 73, 778–786.
- Claiborne, B.J., Amaral, D.G., and Cowan, W.M. (1986). A light and electron microscopic analysis of the mossy fibers of the rat dentate gyrus. *J. Comp. Neurol.* 246, 435–458.
- Edri, R., Yaffe, Y., Ziller, M.J., Mutukula, N., Volkman, R., David, E., Jacob-Hirsch, J., Malcov, H., Levy, C., Rechavi, G., et al. (2015). Analysing human neural stem cell ontogeny by consecutive isolation of Notch active neural progenitors. *Nat. Commun.* 6, 6500.
- Eiraku, M., Takata, N., Ishibashi, H., Kawada, M., Sakakura, E., Okuda, S., Sekiguchi, K., Adachi, T., and Sasai, Y. (2011). Self-organizing optic-cup morphogenesis in three-dimensional culture. *Nature* 472, 51–56.
- Eriksson, P.S., Perfilieva, E., Björk-Eriksson, T., Alborn, A.-M., Nordborg, C., Peterson, D.A., and Gage, F.H. (1998). Neurogenesis in the adult human hippocampus. *Nat. Med.* 4, 1313–1317.
- Espuny-Camacho, I., Michelsen, K.A., Gall, D., Linaro, D., Hasche, A., Bonnefont, J., Bali, C., Orduz, D., Bilheu, A., Herpoel, A., et al. (2013). Pyramidal neurons derived from human pluripotent stem cells integrate efficiently into mouse brain circuits in vivo. *Neuron* 77, 440–456.
- Falkner, S., Grade, S., Dimou, L., Conzelmann, K.-K., Bonhoeffer, T., Götz, M., and Hübener, M. (2016). Transplanted embryonic neurons integrate into adult neocortical circuits. *Nature* 539, 248–253.
- Fricker-Gates, R.A., Shin, J.J., Tai, C.C., Catapano, L.A., and Macklis, J.D. (2002). Late-stage immature neocortical neurons reconstruct interhemispheric connections and form synaptic contacts with increased efficiency in adult mouse cortex undergoing targeted neurodegeneration. *J. Neurosci.* 22, 4045–4056.
- Fukuchi-Shimogori, T., and Grove, E.A. (2003). Emx2 patterns the neocortex by regulating FGF positional signaling. *Nat. Neurosci.* 6, 825–831.
- Gaarskjaer, F.B. (1978). Organization of the mossy fiber system of the rat studied in extended hippocampi. *J. Comp. Neurol.* 178, 73–88.
- Gage, F.H., Coates, P.W., Palmer, T.D., Kuhn, H.G., Fisher, L.J., Suhonen, J.O., Peterson, D.A., Suhr, S.T., and Ray, J. (1995). Survival and differentiation of adult neuronal progenitor cells transplanted to the adult brain. *Proc. Natl. Acad. Sci. USA* 92, 11879–11883.
- Gaillard, A., Prestoz, L., Dumartin, B., Cantereau, A., Morel, F., Roger, M., and Jaber, M. (2007). Reestablishment of damaged adult motor pathways by grafted embryonic cortical neurons. *Nat. Neurosci.* 10, 1294–1299.
- George, P.M., and Steinberg, G.K. (2015). Novel stroke therapeutics: unraveling stroke pathophysiology and its impact on clinical treatments. *Neuron* 87, 297–309.
- Guitet, J., Garnier, C., Ebrahimi-Gaillard, A., and Roger, M. (1994). Efferents of frontal or occipital cortex grafted into adult rat's motor cortex. *Neurosci. Lett.* 180, 265–268.
- Gyorgy, A.B., Szemes, M., de Juan Romero, C., Tarabykin, V., and Agoston, D.V. (2008). SATB2 interacts with chromatin-remodeling molecules in differentiating cortical neurons. *Eur. J. Neurosci.* 27, 865–873.
- Hansen, D.V., Rubenstein, J.L.R., and Kriegstein, A.R. (2011). Deriving excitatory neurons of the neocortex from pluripotent stem cells. *Neuron* 70, 645–660.
- Hébert, J.M., and McConnell, S.K. (2000). Targeting of cre to the Foxg1 (BF-1) locus mediates loxP recombination in the telencephalon and other developing head structures. *Dev. Biol.* 222, 296–306.
- Hiragi, T., Andoh, M., Araki, T., Shirakawa, T., Ono, T., Koyama, R., and Ikegaya, Y. (2017). Differentiation of human induced pluripotent stem cell (hiPSC)-derived neurons in mouse hippocampal slice cultures. *Front. Cell. Neurosci.* 11, 143.
- Imayoshi, I., Shimogori, T., Ohtsuka, T., and Kageyama, R. (2008). Hes genes and neurogenin regulate non-neural versus neural fate specification in the dorsal telencephalic midline. *Development* 135, 2531–2541.
- Iqbal, K., Liu, F., and Gong, C. (2015). Tau and neurodegenerative disease: the story so far. *Nat. Rev. Neurol.* 12, 15–27.
- Kuwamura, M., Muraguchi, T., Matsui, T., Ueno, M., Takenaka, S., Yamate, J., Kotani, T., Kuramoto, T., Guénet, J.-L., Kitada, K., et al. (2005). Mutation at the Lmx1a locus provokes aberrant brain development in the rat. *Dev. Brain Res.* 155, 99–106.
- Kwan, K.M., Fujimoto, E., Grabher, C., Mangum, B.D., Hardy, M.E., Campbell, D.S., Parant, J.M., Yost, H.J., Kanki, J.P., and Chien, C.B. (2007). The Tol2kit: a multisite gateway-based construction kit for Tol2 transposon transgenesis constructs. *Dev. Dyn.* 236, 3088–3099.
- Lai, S., Panarese, A., Spalletti, C., Alia, C., Ghionzoli, A., Caleo, M., and Micera, S. (2015). Quantitative kinematic characterization of reaching impairments in mice after a stroke. *Neurorehabil. Neural Repair* 29, 382–392.
- Lee, S.H., Lumelsky, N., Studer, L., Auerbach, J.M., and McKay, R.D. (2000). Efficient generation of midbrain and hindbrain neurons from mouse embryonic stem cells. *Nat. Biotechnol.* 18, 675–679.



- Lee, S.T., Chu, K., Jung, K.H., Kim, S.J., Kim, D.H., Kang, K.M., Hong, N.H., Kim, J.H., Ban, J.J., Park, H.K., et al. (2008). Anti-inflammatory mechanism of intravascular neural stem cell transplantation in haemorrhagic stroke. *Brain* *131*, 616–629.
- Lupo, G., Bertacchi, M., Carucci, N., Augusti-Tocco, G., Biagioni, S., and Cremisi, F. (2014). From pluripotency to forebrain patterning: an in vitro journey astride embryonic stem cells. *Cell. Mol. Life Sci.* *71*, 2917–2930.
- Machon, O., Backman, M., Machonova, O., Kozmik, Z., Vacik, T., Andersen, L., and Krauss, S. (2007). A dynamic gradient of Wnt signaling controls initiation of neurogenesis in the mammalian cortex and cellular specification in the hippocampus. *Dev. Biol.* *311*, 223–237.
- Magavi, S.S., Leavitt, B.R., and Macklis, J.D. (2000). Induction of neurogenesis in the neocortex of adult mice. *Nature* *405*, 951–955.
- Mariani, J., Simonini, M.V., Palejev, D., Tomasini, L., Coppola, G., Szekely, A.M., Horvath, T.L., and Vaccarino, M.V. (2012). Modeling human cortical development in vitro using induced pluripotent stem cells. *Proc. Natl. Acad. Sci. USA* *109*, 12770–12775.
- Michelsen, K.A., Acosta-verdugo, S., Benoit-marand, M., Espuny-camacho, I., Gaspard, N., Saha, B., Gaillard, A., and Vanderhaeghen, P. (2015). Area-specific reestablishment of damaged circuits in the adult cerebral cortex by cortical neurons derived from mouse embryonic stem cells. *Neuron* *85*, 982–997.
- Millonig, J.H., Millen, K.J., and Hatten, M.E. (2000). The mouse Dreher gene *Lmx1a* controls formation of the roof plate in the vertebrate CNS. *Nature* *403*, 764–769.
- Modo, M., Stroemer, R.P., Tang, E., Patel, S., and Hodges, H. (2002). Effects of implantation site of stem cell grafts on behavioral recovery from stroke damage. *Stroke* *33*, 2270–2278.
- Monuki, E.S., Porter, F.D., and Walsh, C.A. (2001). Patterning of the dorsal telencephalon and cerebral cortex by a roof plate-*Lhx2* pathway. *Neuron* *32*, 591–604.
- Nielsen, J.V., Blom, J.B., Noraberg, J., and Jensen, N.A. (2010). *Zbtb20*-Induced CA1 pyramidal neuron development and area enlargement in the cerebral midline cortex of mice. *Cereb. Cortex* *20*, 1904–1914.
- Poewe, W., Seppi, K., Tanner, C.M., Halliday, G.M., Brundin, P., Volkman, J., Schrag, A.-E., and Lang, A.E. (2017). Parkinson disease. *Nat. Rev. Dis. Primers* *3*, 17013.
- Rosario, C.M., Yandava, B.D., Kosaras, B., Zurakowski, D., Sidman, R.L., and Snyder, E.Y. (1997). Differentiation of engrafted multipotent neural progenitors towards replacement of missing granule neurons in meander tail cerebellum may help determine the locus of mutant gene action. *Development* *124*, 4213–4224.
- Sheen, V.L., Arnold, M.W., Wang, Y., and Macklis, J.D. (1999). Neural precursor differentiation following transplantation into neocortex is dependent on intrinsic developmental state and receptor competence. *Exp. Neurol.* *158*, 47–62.
- Shetty, A.K., and Turner, D.A. (1996). Development of fetal hippocampal grafts in intact and lesioned hippocampus. *Prog. Neurobiol.* *50*, 597–653.
- Shi, Y., Kirwan, P., Smith, J., Robinson, H.P.C., and Livesey, F.J. (2012). Human cerebral cortex development from pluripotent stem cells to functional excitatory synapses. *Nat. Neurosci.* *15*, 477–486.
- Shin, J.J., Fricker-Gates, R.A., Perez, F.A., Leavitt, B.R., Zurakowski, D., and Macklis, J.D. (2000). Transplanted neuroblasts differentiate appropriately into projection neurons with correct neurotransmitter and receptor phenotype in neocortex undergoing targeted projection neuron degeneration. *J. Neurosci.* *20*, 7404–7416.
- Shiraishi, A., Muguruma, K., and Sasai, Y. (2017). Generation of thalamic neurons from mouse embryonic stem cells. *Development* *144*, 1211–1220.
- Sloviter, R.S. (1989). Calcium-binding protein (calbindin-D28k) and parvalbumin immunocytochemistry: localization in the rat hippocampus with specific reference to the selective vulnerability of hippocampal neurons to seizure activity. *J. Comp. Neurol.* *280*, 183–196.
- Subramanian, L., Remedios, R., Shetty, A., and Tole, S. (2009). Signals from the edges: the cortical hem and antihem in telencephalic development. *Semin. Cell Dev. Biol.* *20*, 712–718.
- Swanson, L.W., Wyss, J.M., and Cowan, W.M. (1978). An autoradiographic study of the organization of intrahippocampal association pathways in the rat. *J. Comp. Neurol.* *181*, 681–715.
- Theil, T., Aydin, S., Koch, S., Grotewold, L., and Rütger, U. (2002). Wnt and Bmp signalling cooperatively regulate graded *Emx2* expression in the dorsal telencephalon. *Development* *129*, 3045–3054.
- Tornero, D., Wattananit, S., Madsen, M.G., Koch, P., Wood, J., Tatarishvili, J., Mine, Y., Ge, R., Monni, E., Devaraju, K., et al. (2013). Human induced pluripotent stem cell-derived cortical neurons integrate in stroke-injured cortex and improve functional recovery. *Brain* *136*, 3561–3577.
- Van de Leemput, J., Boles, N.C., Kiehl, T.R., Corneo, B., Lederman, P., Menon, V., Lee, C., Martinez, R.A., Levi, B.P., Thompson, C.L., et al. (2014). CORTECON: a temporal transcriptome analysis of in vitro human cerebral cortex development from human embryonic stem cells. *Neuron* *83*, 51–68.
- Van Praag, H., Schinder, A.F., Christie, B.R., Toni, N., Palmer, T.D., and Gage, F.H. (2002). Functional neurogenesis in the adult hippocampus. *Nature* *415*, 1030–1034.
- Yao, Z., Mich, J.K., Ku, S., Menon, V., Krostag, A.R., Martinez, R.A., Furchtgott, L., Mulholland, H., Bort, S., Fuqua, M.A., et al. (2017). A single-cell roadmap of lineage bifurcation in human ESC models of embryonic brain development. *Cell Stem Cell* *20*, 120–134.
- Yoshida, M., Suda, Y., Matsuo, I., Miyamoto, N., Takeda, N., Kuratani, S., and Aizawa, S. (1997). *Emx1* and *Emx2* functions in development of dorsal telencephalon. *Development* *124*, 101–111.
- Yu, D.X., Di Giorgio, F.P., Yao, J., Marchetto, M.C., Brennand, K., Wright, R., Mei, A., McHenry, L., Lisuk, D., Grasmick, J.M., et al. (2014). Modeling hippocampal neurogenesis using human pluripotent stem cells. *Stem Cell Reports* *2*, 295–310.
- Zaman, V., and Shetty, A.K. (2001). Fetal hippocampal CA3 cell grafts transplanted to lesioned CA3 region of the adult hippocampus exhibit long-term survival in a rat model of temporal lobe epilepsy. *Neurobiol. Dis.* *8*, 942–952.